Supplementary information

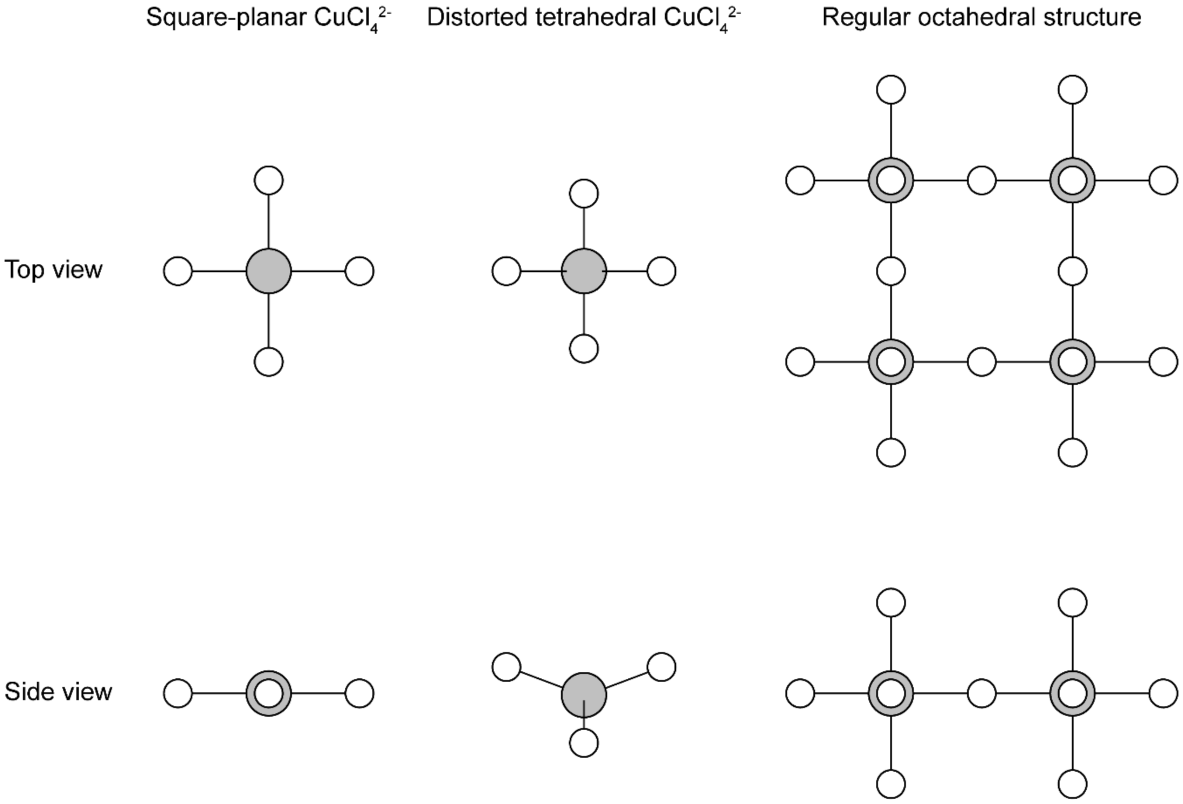

Figure S1: Schematic with examples of the square-planar, distorted tetrahedral and octahedral geometries in top view (top) and side view (bottom). In the case of the distorted tetrahedral geometry the angles between neighboring chloride ions are not necessarily 90°.

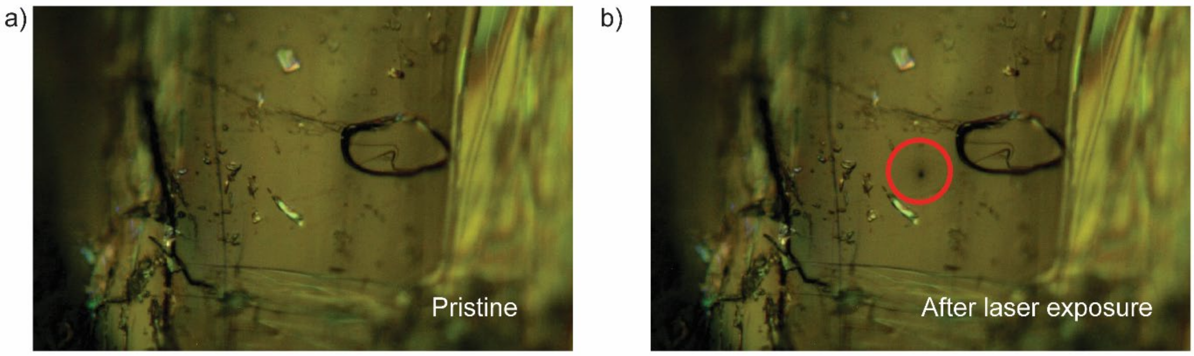

Figure S2: Microscope images of a $(PEA)_2CuCl_4$ single crystal before a) and after b) extended laser exposure (532 nm) with the Raman setup. The laser induces the color change to brown locally; the dark spot indicated by the red circle is an example of the conversion.

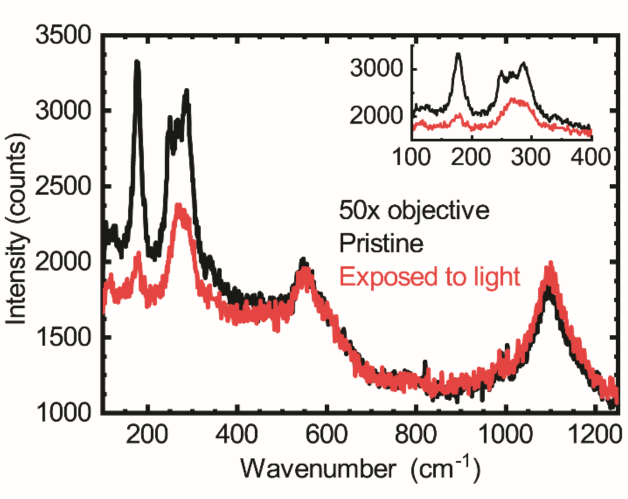

Figure S3: Raman spectra of a pristine $(PEA)_2CuCl_4$ thin film (black line) and after exposure to UV light (red line), made with a 50x objective. The wavelength of the laser was 532 nm. The inset shows the region between 100 and 400 cm^{-1}. Differences with respect to the single crystal data of the main text, the pronounced peak around 1100 cm^{-1}, for example, are due to contributions from the glass substrate.

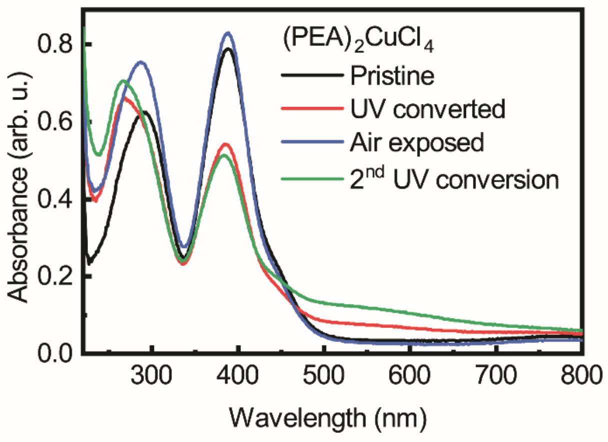

Figure S4: Thin film absorbance spectra of $(PEA)_2CuCl_4$ in the case of a pristine film (black line) and after 45 minutes of UV illumination in nitrogen environment (red line). The sample was kept in air for 22 days (blue line), and illuminated with UV for 45 minutes in nitrogen afterwards (green line). The pristine measurement was carried out on a different film to make sure that the material was not in contact with air before UV treatment. The second UV conversion shows the reversibility of the photochromism in $(PEA)_2CuCl_4$, the spectrum is very similar to that after the first UV treatment (apart from some intensity variations).

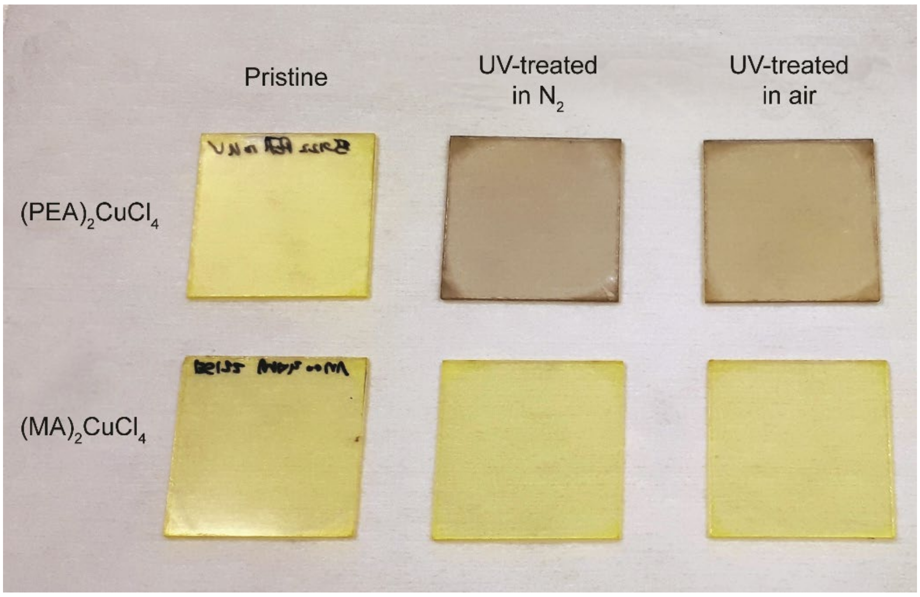

Figure S5: Photograph of $(PEA)_2CuCl_4$ *(top row) and* $(MA)_2CuCl_4$ *(bottom row) thin films. These films are pristine (first column), UV-treated in* N_2 *(second column) and UV-treated in air (third column). UV treatment was carried out with* $\lambda = 312$ *nm. This shows that* $(PEA)_2CuCl_4$ *can change to the brown phase in air.*

Photochromism in $(PEA)_2CuCl_4$: the role of the light's wavelength and the atmosphere

From Figure 1a (λ = 254 nm) and Figure S5 (λ = 312 nm) it becomes clear that the atmosphere and the wavelength of the UV light used for the conversion are crucial for the process. UV-treatment of $(PEA)_2CuCl_4$ in nitrogen always results in a conversion to the brown phase, whereas illumination in air only leads to conversion with λ = 312 nm light. This anomaly might hint at competing mechanisms and remains under investigation.

We studied the influence of the wavelength of the light by using a white light source with bandpass filters (full width at half maximum 10±2 nm) to expose the film in air. The light was focused on the film by using a set of lenses, leading a spot of approximately 3 mm in diameter. This allowed us to see the effect of visible light (400 – 600 nm) on $(PEA)_2CuCl_4$. We found that focused light with a wavelength shorter than 480 nm converts the film to the brown phase. This coincides with the ligand-to-metal charge transfer energy of the material (Figure 1b).

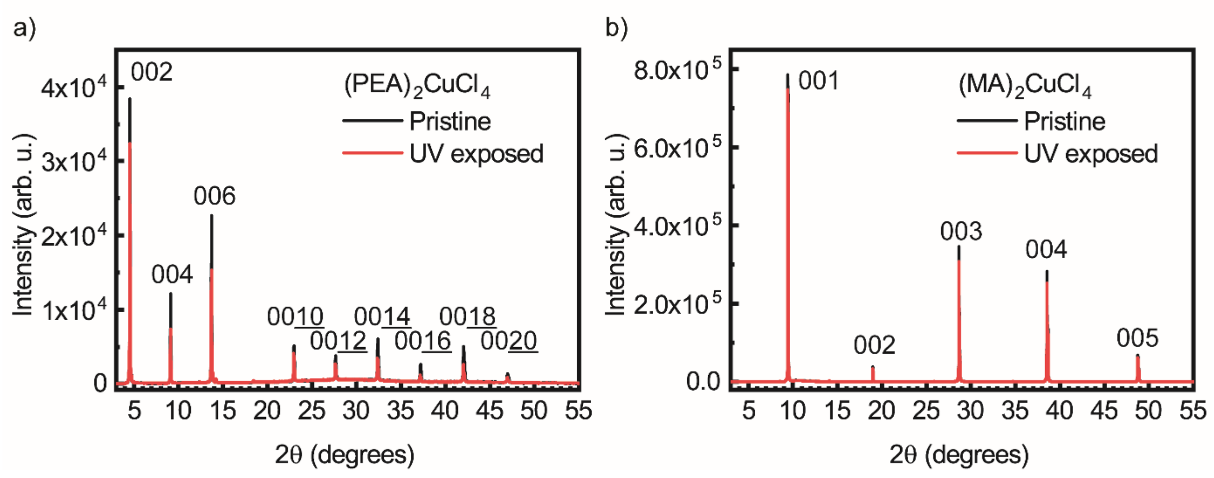

Figure S6: Indexed powder XRD patterns of thin films of a) $(PEA)_2CuCl_4$ and b) $(MA)_2CuCl_4$, both pristine and after UV exposure.

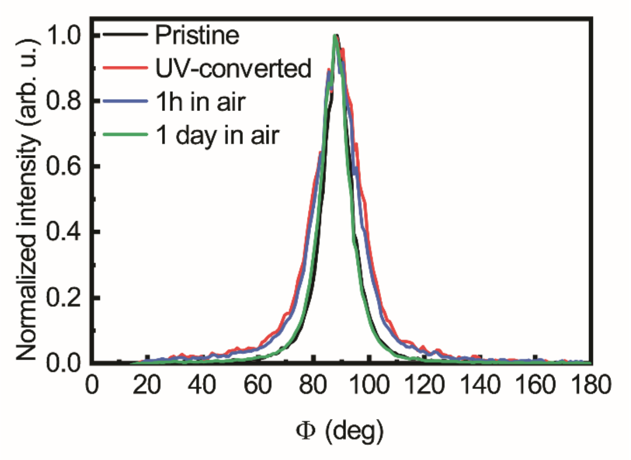

Figure S7: Comparison of the normalized azimuthal intensity profiles of the 002 reflection for the pristine (black line) and UV-converted (red line) (PEA)2CuCl4 film, and for the film after 1h in air (blue line) and 1 day in air (green line). These profiles are extracted from the GIWAXS data in Figure 4. It can be seen that the pristine sample has a high degree of alignment with an angular spreading of only ± 6 deg. Interestingly, upon UV exposure, the angular spreading increases to ± 10 deg. This is a further confirmation that UV conversion causes structural disorder and structural rearrangement. As observed for the 113 reflection, the effect is reversible and after 1 day, the degree of structural alignment is fully recovered.

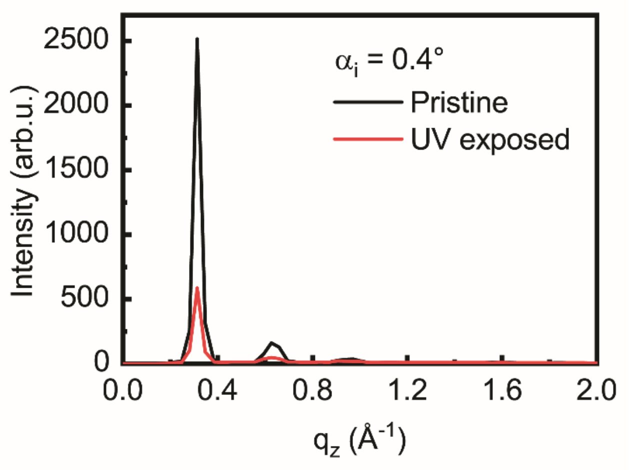

Figure S8: Comparison of the GIWAXS intensity linecuts for the pristine and irradiated samples along the quasi-vertical q_z direction. The incident angle was 0.4°.

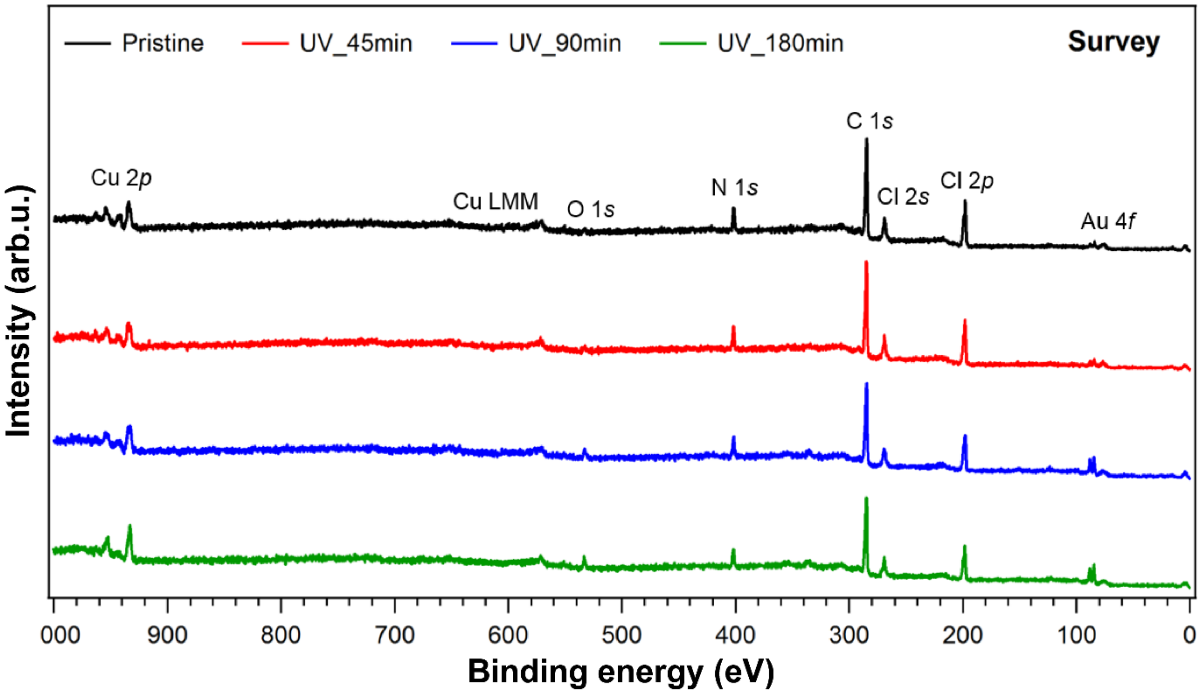

Figure S9: XPS survey spectra of the (PEA)$_2$CuCl$_4$ film before (black line) and after UV illumination. The spectra of UV-treated (PEA)$_2$CuCl$_4$ are shown in red (45 min total duration), blue (90 min) and green (180 min).

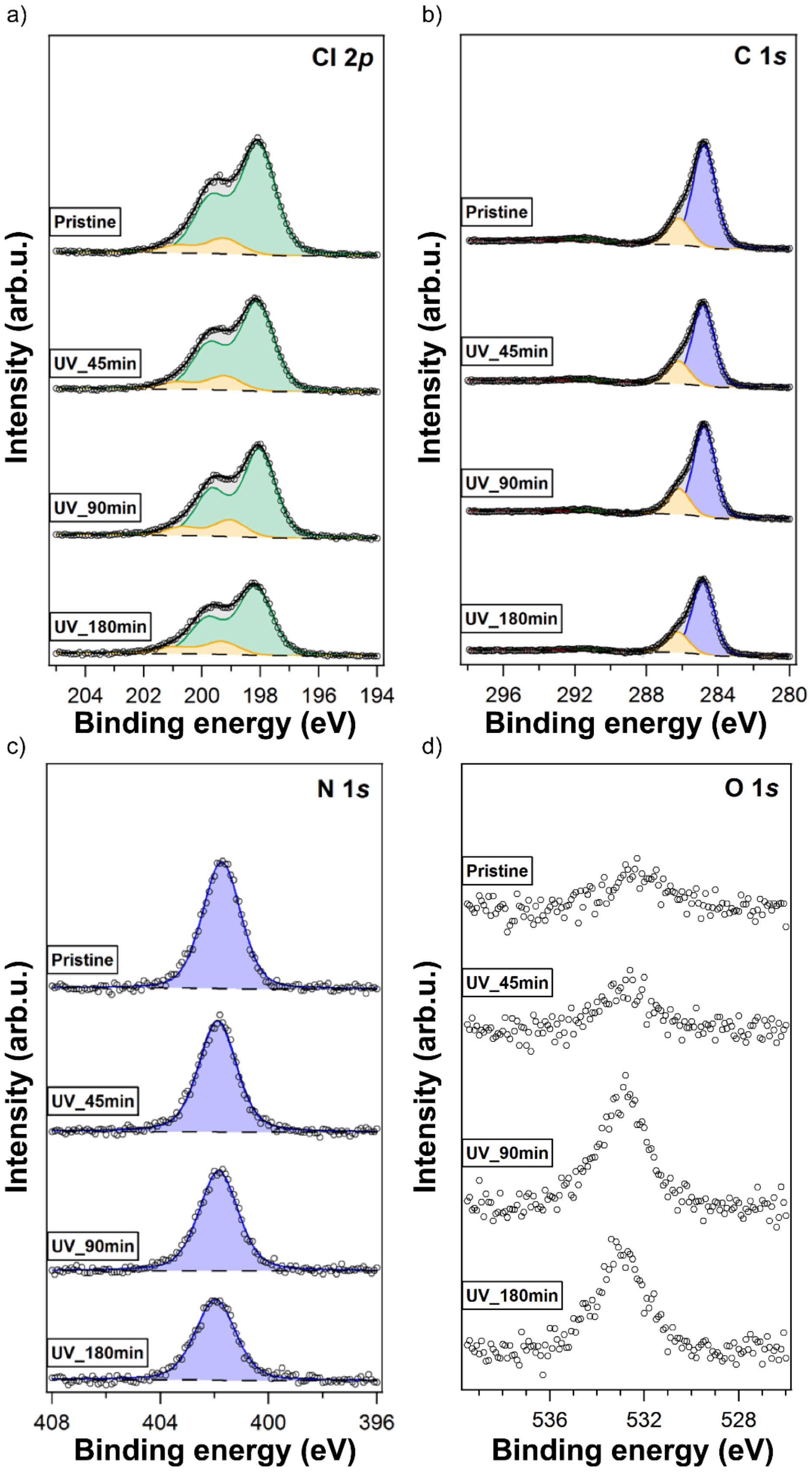

Figure S10: High-resolution XPS spectra of a) Cl 2p, b) C 1s, c) N 1s and d) O 1s for the pristine material and after the three UV-treatments.

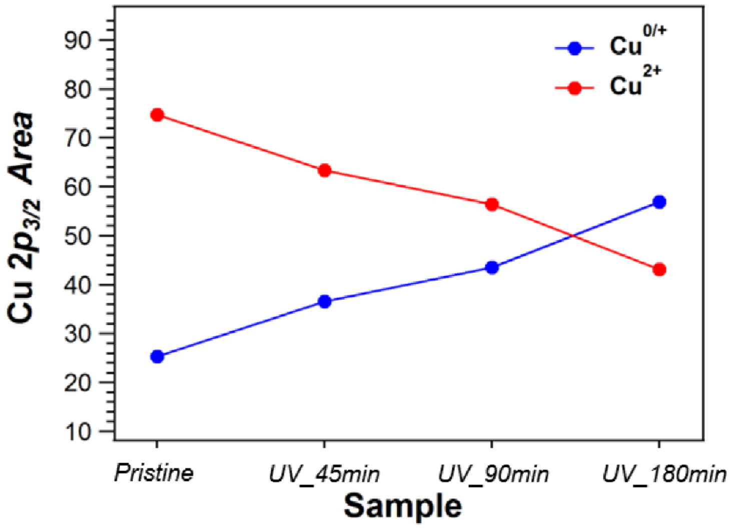

Figure S11: Variation of the relative intensities of the two components attributed to Cu^{2+} and $Cu^{0/+}$ over the course of the UV treatment.

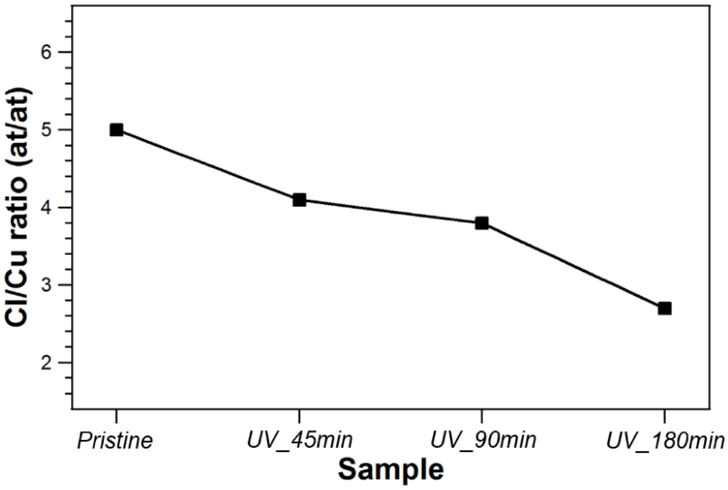

Figure S12: Cl/Cu atomic ratio over the course of the UV treatment.